Indian Geotechnical Journal, 39(4), October 2009, 436-452

TECHNICAL NOTE

Experimental Study of Horizontal Vibration of Footing on Dry Cohesionless Soil

Sanjay Paul* and Ashim Kanti Dey**

Introduction

The problems associated with foundations resisting dynamic loads either from the supported machinery or from the external sources require special solutions considering local soil conditions and environment. The foundation must satisfy stability under dynamic loading as well as static loading conditions.

The dynamic load generated by natural forces from earthquakes, wind, traffic, blasting and neighboring machinery may be transmitted to the foundation through a structural system or through the soil. In most of these cases, it is necessary to obtain field measurements under the loading conditions expected to be encountered by the prototype. In the last decade, a number of model tests (Al Homoud, et. al.,1996; Liu and Dobry,1997; Maugeria et. al.,2000; Knappett, et. al.,2006) were performed to simulate the behavior of shallow foundations under earthquake forces. Earlier, the dynamic behaviour of foundations had been studied by Barkan (1962), Prakash (1981) and others. The authors also carried out a study on the behavior of shallow foundations under seismic forces (Paul and Dey, 2005).

The present research concentrates on the influence on horizontal vibration response of model footings on sand by the parameters, horizontal acceleration coefficients of footing (k_{hf}), horizontal acceleration coefficients of sand (k_{hs}), shape of footing, footing embedment depth and the void ratio of sand. The present study uses dry fine sand from Silchar, India.

Methodology

Seismic effects on shallow foundations are usually analysed by pseudo-static approach in which the effects of earthquake forces are accounted by constant horizontal and vertical accelerations attached to the inertia. The common form of pseudo-static analyses considers the effects of earthquake shaking by pseudo-static accelerations that produce inertial forces, F_h and F_v, which act through the centroid of the failure mass in the horizontal and vertical directions respectively. The magnitudes of the pseudo-static forces are as follows.

* Research Scholar, Department of Civil Engineering, National Institute of Technology, Silchar – 788 010, India, e-mail: sanjaypaul_76@yahoo.com

** Professor, Department of Civil Engineering, National Institute of Technology, Silchar – 788 010, India, e-mail: ashim_kanti@yahoo.co.in

$$F_h = a_h w / g = k_h w \quad (1)$$

$$F_v = a_v w / g = k_v w \quad (2)$$

where a_h and a_v are the horizontal and vertical pseudo-static accelerations, k_h and k_v are the coefficients of the horizontal and vertical pseudo-static accelerations and *W* is the weight of the failure mass.

In the present analysis, the horizontal acceleration coefficient of soil mass (k_{hs}), horizontal acceleration coefficient of footing (k_{hf}) and horizontal acceleration coefficient of tank as input motion (k_{hi}) are correlated. The term k_{hs} ,k_{hf} and k_{hi} can be obtained as :

$$K_{hs} = a_{hs} / g \quad (3)$$

$$khf = ahf / g \quad (4)$$

$$k_{hi} = a_{hi} / g \quad (5)$$

where, a_{hs} , a_{hf} and a_{hi} are the accelerations acted upon by the seismic forces on soil mass, footing and tank as input motions respectively.

The correlations can be expressed as,

$$k_{hf} = a.k_{hi} + b \quad (6)$$

$$k_{hf} = c.k_{hs} + d \quad (7)$$

where *a*, *b*, *c* and *d* are constants.

Experimental Program

Soil Sampling and Characterization

Representative sample of sand was collected from Silchar town of north-east India. Figure 1 shows the typical grain size distribution of sand sample.

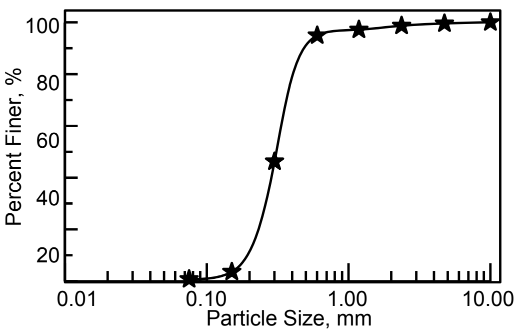

Fig. 1 Grain Size Distribution of Sand used in the Study

Table 1 gives other physical properties of the sand (Paul and Dey, 2006). Experiments were conducted at three different densities of sand sample, viz, 14.72 kN/m^3, 14.44 kN/m^3 and 14.26 kN/m^3. Corresponding void ratios are 0.76, 0.80 and 0.82 respectively.

Table 1 Physical Properties of Sand Sample

G_s	2.65
e_{max}	0.93
e_{min}	0.57
D_{10} (mm)	0.19
D_{30} (mm)	0.26
D_{60} (mm)	0.35
C_u	1.84
C_c	1.02

Test Set-up

Figure 2(a) shows the model tank made of mild steel of inside dimension 1.50 m (length) x 0.60 m (width) x 0.90 m (height) with wall thickness of 4 mm. The tank is connected to a 3-phase AC motor of 1.5 HP capacity by a slider crank mechanism (Figure 2(b)). The speed of the motor is 1440 rpm, whereas the speed of the sinusoidal movement of the tank is observed to be 32 rpm, the corresponding frequencies of motor and tank are respectively 24.00 Hz and 0.53 Hz. The amplitude of movement of the tank can be varied by pinning the slider arm at different slots on a 30.5 cm diameter wheel connected to the motor. In the present analysis the amplitude of the to and fro movement of tank is maintained at 29 cm horizontally. The depth of dry sand layer in each experiment was taken as 0.62 m.

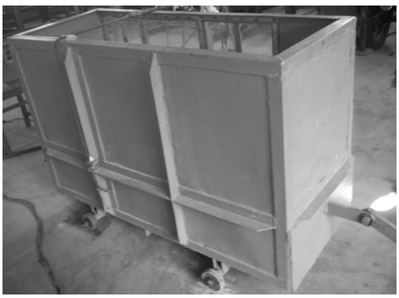

(a) Model Tank of Mild Steel having Inside Dimensions 1.50m (Length) X 0.60m (width) X 0.90m (Height)

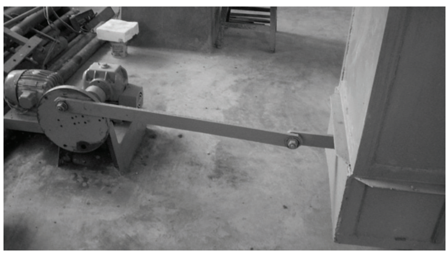

(b) Slider Crank Mechanism for the Connection between Motor and Tank

Fig. 2 Experimental Set-up for Horizontal Vibration Testing

Model Footings

Three model footings were made from mild steel under this study. The dimension and weight of each model are presented in Table 2 and placements of models are shown in Figures 3(a), (b) and (c).

Table 2 Geometry and weight of Mild Steel Footing Models

Base Shape	Base Width (cm)	Base Length (cm)	Height (cm)	Weight (kg)	Symbol
Wide-Strip Footing	12.5	53.0	11.0	8.092	S1
Narrow-Strip Footing	7.5	53.0	5.3	3.750	S2
Rectangular	13.0	15.0	21.0	2.289	R

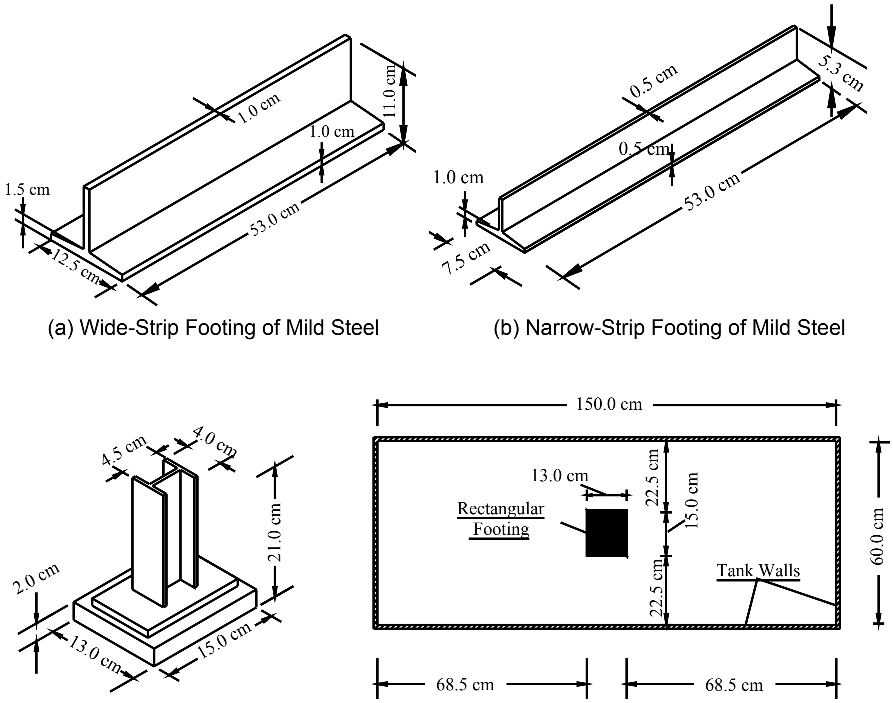

(a) Wide-Strip Footing of Mild Steel (b) Narrow-Strip Footing of Mild Steel

(c) Rectangular Footing of Mild Steel (d) Placement of Rectangular Footing inside the Tank

Fig. 3 Model Footings used in the Present Study

In order to minimize the boundary effects, the width of the tank was made equal to four times the length of the rectangular footing (Figure 3(d)). For the strip footings a clear gap of 3.5 cm was maintained between the tank wall and the edge of the footing considering the actual field problems, where, either the strip footing butts to the original ground stratum or is restrained due to cross strip footings. However, little boundary effects in the observed values are admitted in the present study.

Record of Acceleration-Time History of Model Tests

The acceleration-time histories of model tests were recorded with the help of B & K make FFT analyzer. DeltaTron piezoelectric type sensors were used to record the acceleration. The data were captured in a PC using the software PULSE

Labshop version 10, B & K make (Brüel and Kjaer, 2003). Accelerometers were fixed on the face of the footing, on the soil surface and on the side of the tank .

Testing Procedure

Acceleration –Time histories of soil and footings were recorded for 20 seconds duration by the accelerometers at three different densities of soils, viz., 14.72 kN/m^3, 14.44 kN/m^3 and 14.26 kN/m^3, corresponding relative densities being 27.41%, 35.83% and 45.57% respectively for three different footings, viz., *S1*,*S2* and *R* (Table 2). Each of the three model footings was placed at three embedment conditions, viz., *D/B* = 0.00, 0.25 and 0.50. So, a total of twenty seven tests were performed. Also, at the end of each test, horizontal and vertical displacements along the centre line of each footing was measured manually.

In addition to the above tests, three tests were conducted keeping the sensors on the face of the footing marked *S1* for three different void ratios at an embedment ratio (*D/B*) of 0.00.

Results and Discussions

Effect of Void ratio on the Acceleration Coefficients between Tank as Input Motion (k_{hi}) and Footings (k_{hf})

Figure 4 shows the acceleration-time histories for tank and footing vibrations for *e* = 0.76 and *D/B* = 0.00. It is observed that the peak acceleration value for footing is slightly more than that of the tank.

Figure 5 shows the correlation between k_{hi} and k_{hf} . A linear correlation in the form of equation (6) was obtained between k_{hi} and k_{hf} , the constants of the equation are shown in Table 3 for different void ratios. Figure 6 shows relationship between horizontal acceleration coefficients of tank and strip footing *S1* at different void ratios of soil. It is observed that the slope increases with increase in void ratio.

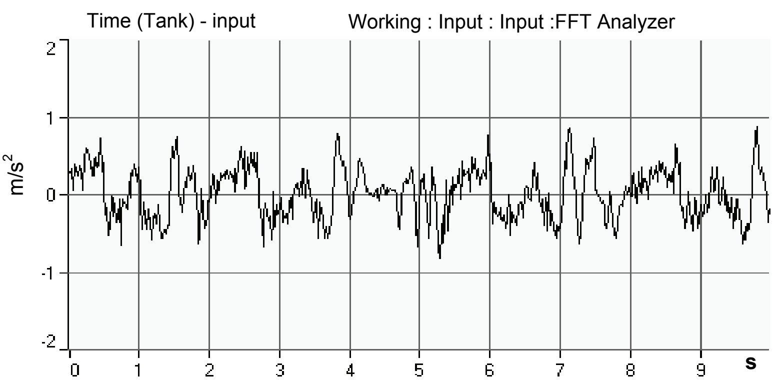

Fig. 4 (a) Typical Acceleration-Time Histories for Wide-Strip Footing with *e* = 0.76 and *D/B* = 0.00 – Tank Vibration as Input Motion

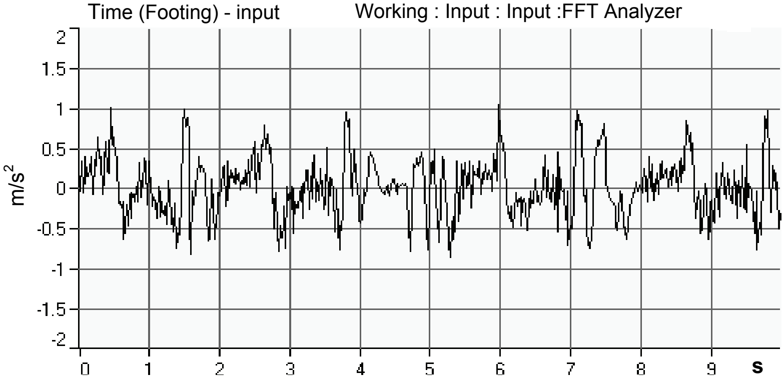

Fig. 4 (b) Typical Acceleration-Time Histories for Wide-Strip Footing with *e* = 0.76 and *D/B* = 0.00 – Footing Response

Table 3 The Values of Coefficients '*a*' and '*b*' used in the Equation (6)

Test No.	Void Ratio (*e*)	Footing	Embedment Ratio (*D/B*)	a	b	R^2
1	0.76	Wide-Strip	0.00	0.959623	0.000071	0.71
2	0.80			1.012175	0.000115	0.79
3	0.82			1.046826	0.000102	0.88

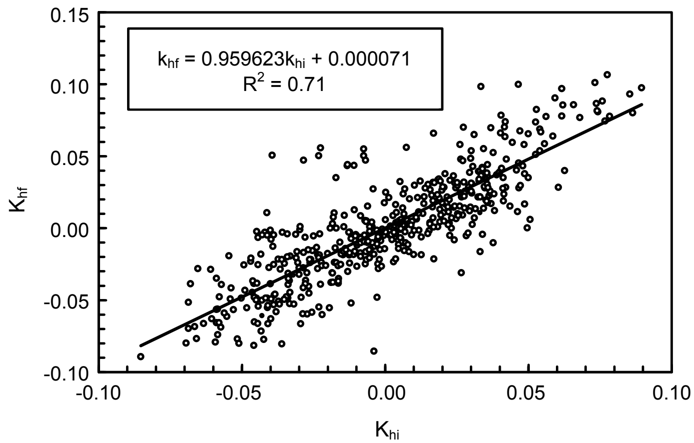

Fig. 5 Typical Correlation between Horizontal Acceleration Coefficients of Tank (k_{hi}) and Wide-Strip Footing (k_{hf}) with *e* = 0.76 and *D/B* = 0.00with e = 0.76 and D/B = 0.00

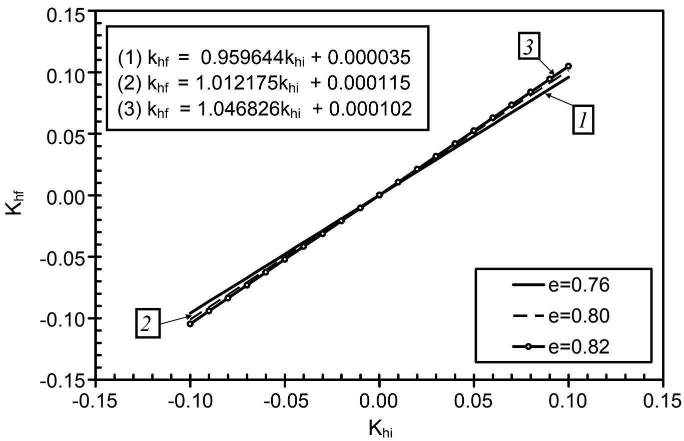

Fig. 6 Correlation between Horizontal Acceleration Coefficients of Tank (*k_{hi}*)and Wide-Strip Footing (*k_{hf}*) with *D/B* = 0.00 at Different Void Ratios

Effect of Void Ratio on the Acceleration Coefficients between Soil (K_{hs}) and those of Footings (K_{hf})

Correlation at Different Embedment Ratios

Figure 7 shows the acceleration-time histories for soil surface and footing vibrations for e = 0.76 and D/B = 0.50. It is observed that the peak acceleration value for footing is slightly more than that for soil deposit. Figure 8 shows the correlation between the same set of acceleration values. Here the best fit line is shown along with it's equation in the form of equation (7) and the acceleration coefficient values are shown in table 4. Figure 9 shows the correlation between horizontal acceleration coefficients of soil (k_{hs}) and footing (k_{hf}) for different *D/B* ratios. It can be seen that as void ratio increases, i.e., as the soil becomes looser, the slope of the best fit line becomes steeper.

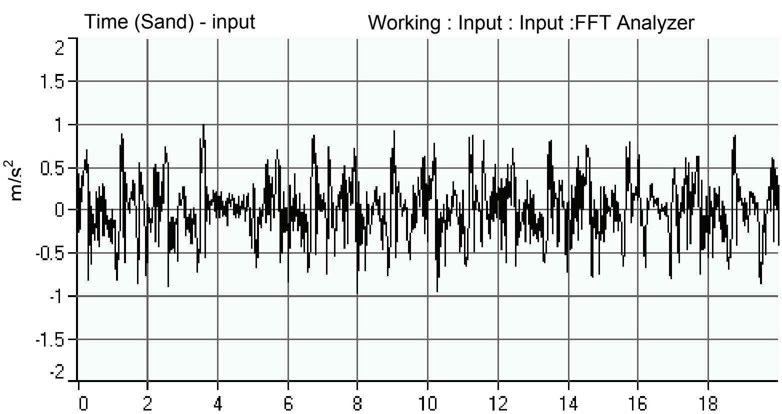

Fig. 7 (a) Typical Acceleration-Time Histories for Wide-Strip Footing with *E* = 0.76 and *D/B* = 0.50 – Soil Response

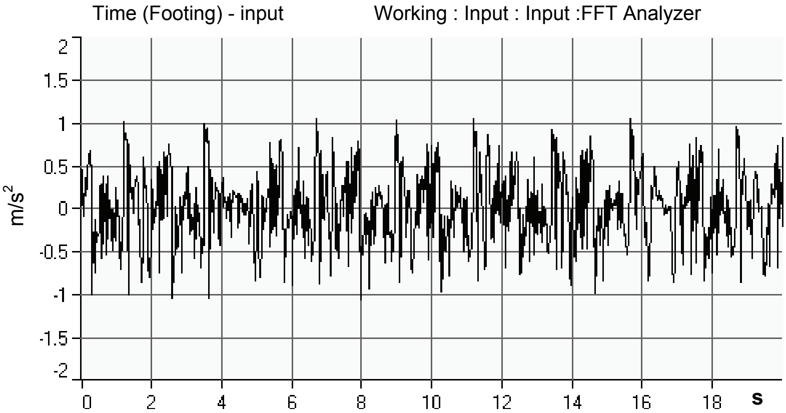

Fig. 7 (b) Typical Acceleration-Time Histories for Wide-Strip Footing with *E* = 0.76 and *D/B* = 0.50 – Footing Response

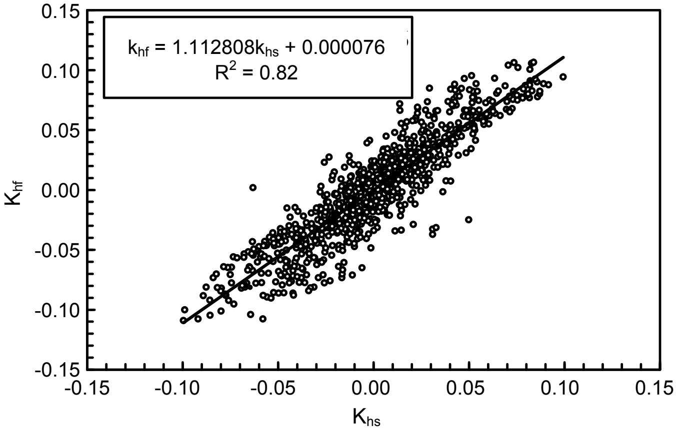

Fig. 8 Typical Correlation between Horizontal Acceleration Coefficients of Soil (k_{hs}) and Wide-Strip Footing (k_{hf}) with *e* = 0.76 and *D/B* = 0.50

Table 4 The Values of Coefficients '*C*' and '*D*' used in the Equation (7)

Test No.	Void Ratio (*e*)	Footing	Embedment Ratio (*D/B*)	c	d	R^2
1	0.76	Wide-Strip	0.00	0.858806	0.000087	0.58
2			0.25	1.011458	0.000091	0.74
3			0.50	1.112808	0.000076	0.82
4		Narrow-Strip	0.00	0.890205	-0.000050	0.62
5			0.25	1.052727	0.000083	0.74
6			0.50	1.130579	-0.000126	0.84
7		Rectangular	0.00	0.832173	0.000044	0.52

Table 4 The Values of Coefficients '*C*' and '*D*' used in the Equation (7) Contd..

Test No.	Void Ratio (*e*)	Footing	Embedment Ratio (*D/B*)	c	d	R^2
8			0.25	1.054096	-0.000159	0.78
9			0.50	1.055540	-0.000073	0.75
10	0.79	Wide-Strip	0.00	0.878347	0.000083	0.72
11			0.25	1.044688	0.000022	0.85
12			0.50	1.004988	-0.000014	0.82
13		Narrow-Strip	0.00	0.958042	0.000050	0.84
14			0.25	1.050903	0.000117	0.84
15			0.50	1.094155	-0.000218	0.92
16		Rectangular	0.00	0.825846	-0.000191	0.59
17			0.25	0.979686	0.000091	0.77
18			0.50	1.064392	0.000004	0.80
19	0.82	Wide-Strip	0.00	0.986076	0.000011	0.85
20			0.25	1.100835	0.000011	0.86
21			0.50	1.083799	0.000054	0.90
22		Narrow-Strip	0.00	1.017182	-0.000023	0.88
23			0.25	1.071827	-0.000043	0.87
24			0.50	1.108473	-0.000025	0.87
25		Rectangular	0.00	0.978847	0.000023	0.70
26			0.25	1.113719	-0.000063	0.79
27			0.50	1.060479	0.000227	0.72

Correlation at Different Footing Types

Figure 10 shows the correlation between horizontal acceleration coefficients of soil (k_{hs}) and footings (k_{hf}) for different void ratios. It is observed that the slope of best fit line is flat for the rectangular footing, whereas it becomes steeper for large-strip footing and becomes the steepest for small-strip footing. Similar observations, as stated above, were obtained for all three void ratios also.

Correlation at Different Void Ratios

Figure 11 shows the correlation between horizontal acceleration coefficients between soil (k_{hs}) and footings (k_{hf}). It can be seen that, as the void ratio increases, i.e., if the soil becomes looser, then the slope of the best fit line becomes steeper.

Generalised Equation

Based on the results given in Table 4**,** the generalized equation containing k_{hf}, k_{hs}, *e*, *D* and *B* can be expressed as follows :

$$k_{hf} = 0.867.k_{hs} + 6.520.e^{31.77} + 0.013.(D/B)^{0.091} \qquad (8)$$

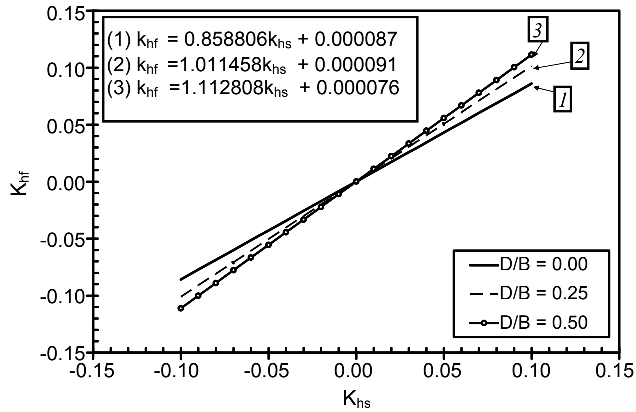

(a) Wide Strip Footing

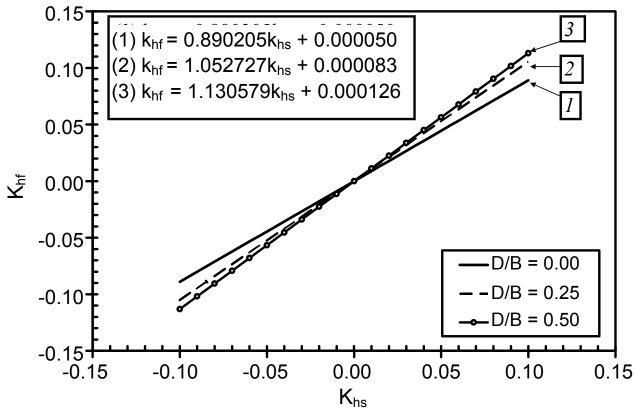

(b) Narrow Strip Footing

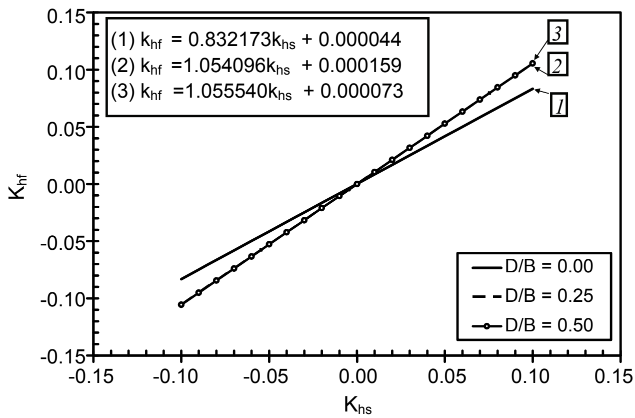

(c) Rectangular Footing

Fig. 9 Correlation between Horizontal Acceleration Coefficients of Soil (k_{hs}) and Different Footings (k_{hf}) with e = 0.76 at Different D/B Ratios

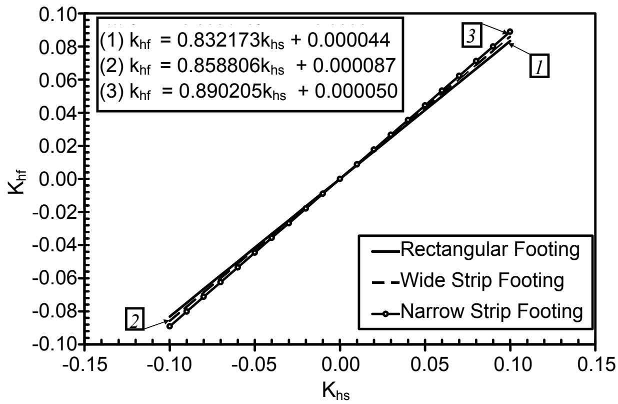

(a) e = 0.76

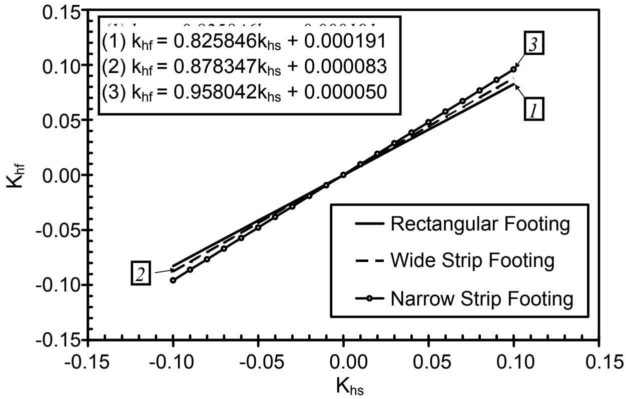

(b) e = 0.80

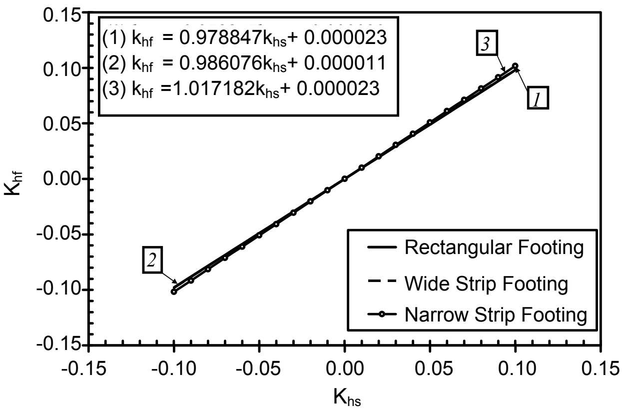

(c) e = 0.82

Fig. 10 Correlation Between Horizontal Acceleration Coefficients of Soil (K_{hs})and Different Footings (K_{hf}) with D/B = 0.00 at Different Void Ratios

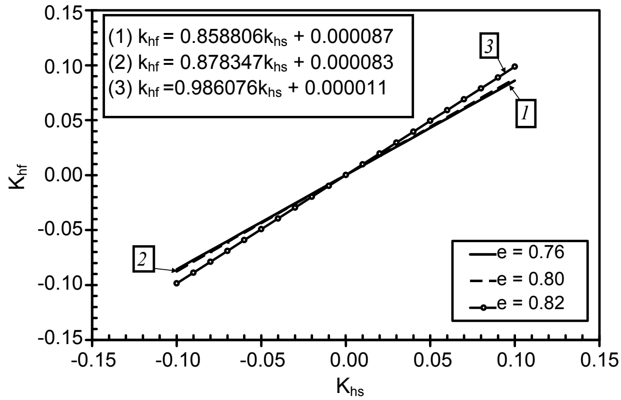

(a) D/B = 0.00

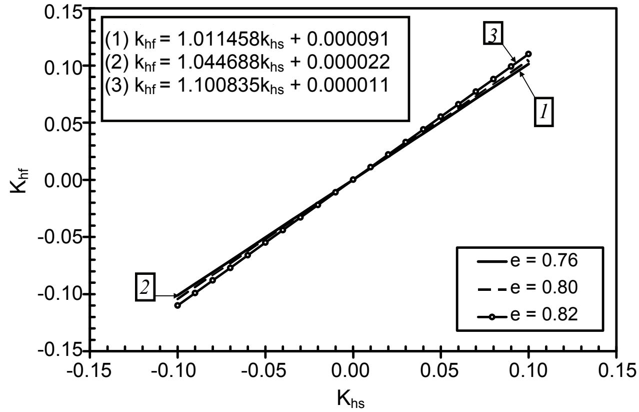

(b) D/B = 0.25

Fig. 11 Correlation between Horizontal Acceleration Coefficients of Soil (K_{hs}) and Footings (K_{hf}) with Wide-Strip Footing at Different Void Ratios and D/B Ratios

Figure 12 shows a typical comparison between observed and calculated k_{hs} values with corresponding R^2 value. From the figure, it can be observed that calculated k_{hs} values of are in good agreement with the observed k_{hs} values.

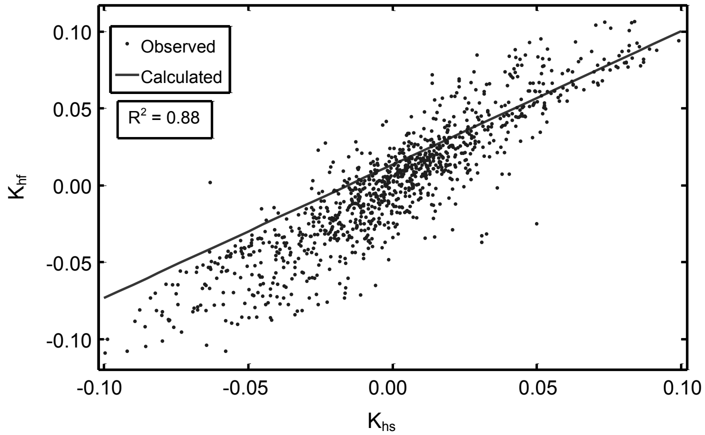

Fig. 12 Comparison between Horizontal Acceleration Coefficients of Soil (K_{hs}) and Footings (K_{hf}) Obtainedby Equation (8) and from Observation with E = 0.76 and Wide-Strip Footing at D/B Ratio of 0.50

Horizontal Displacement of Footing after the Test

Figure 13 shows the horizontal displacement of different footings at different D/B ratios and void ratios. It is observed that the horizontal displacement of footing reduces with the increase of embedment ratio. As expected, the displacement increases with increase in void ratio.

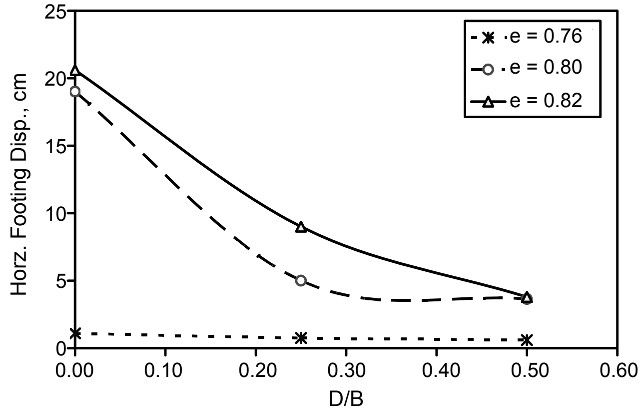

(a) Wide Strip Footing

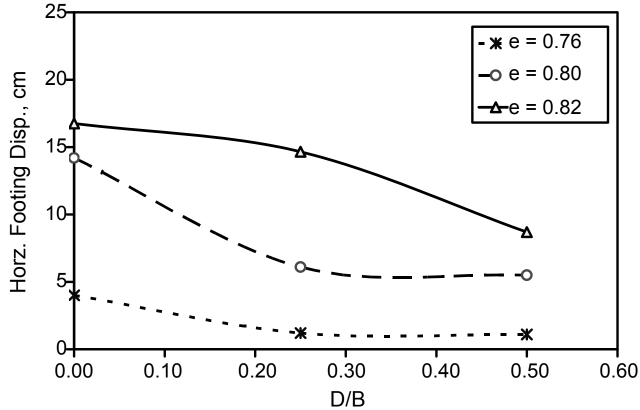

(b) Narrow Strip Footing

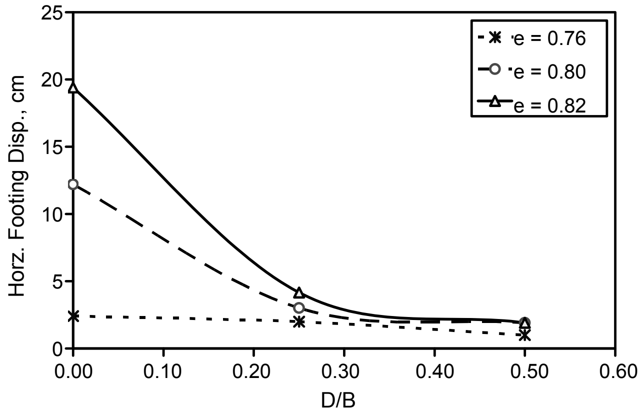

(c) Rectangular Footing

Fig. 13 Variation of Horizontal Displacements of Different Footings with the Variation of Void Ratio and Embedment Ratio

Vertical Displacement of Footing after the Test

Figure 14 shows the vertical displacement of different footings at different *D/B* ratios and void ratios.

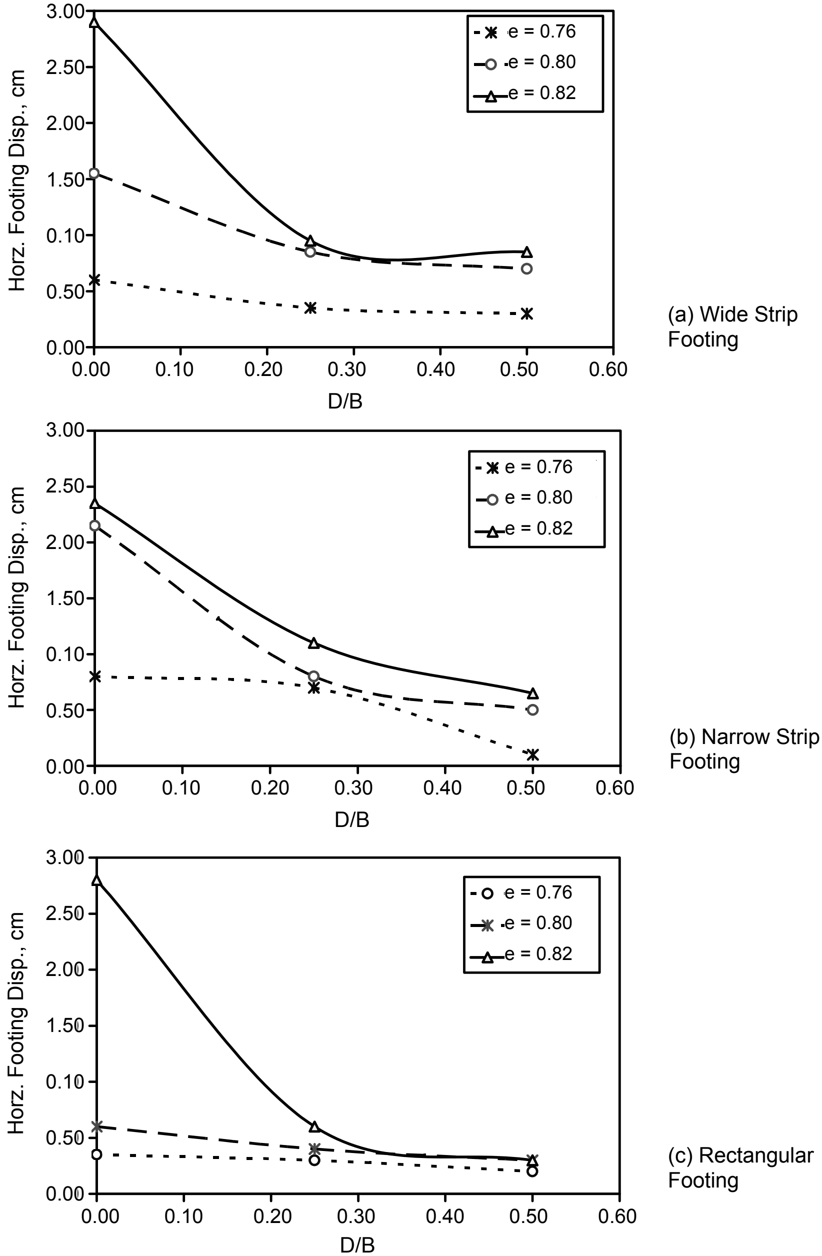

Fig. 14 Variation of Vertical Displacements of Different Footings with the Variation of Void Ratio and Embedment Ratio

It is observed that the vertical displacement of footing reduces with the increase of embedment ratio. This displacement increases with the increase of void ratio for most of the cases.

Conclusions

In the present analysis the horizontal acceleration coefficients of soil mass (k_{hs}), footing (k_{hf}) and tank as input motion (k_{hi}) are correlated. It is observed that the horizontal acceleration coefficient depends upon several parameters like, type of footing, void ratio of soil deposit and embedment ratio of the footing. There exists a linear relationship between the horizontal acceleration coefficients of tank as input motion (k_{hi}) and footing (k_{hf}). It is observed that the slope of the best fit lines increase with increase in void ratio. Again it is observed that there exists a linear relationship between the horizontal acceleration coefficients of soil (k_{hs}) and footing (k_{hf}). It is also also observed that the slope of the best fit lines increase with increase in void ratio. However, the slope of best fit line is flat for the rectangular footing, steeper for big-strip footing and becomes the steepest for small-strip footing. A generalized equation is generated containing k_{hf}, k_{hs}, e, D and B. The calculated k_{hs} values using this equation are in good agreement with the observed k_{hs} values. Total horizontal and vertical displacements of footings after a dynamic load also depend upon the parameters like, type of footing, void ratio of soil deposit and embedment ratio of the footing.

Notations

a, b = Coefficients used in the equation (6)

ah = Horizontal pseudo-static acceleration

a_v = Vertical pseudo-static acceleration

a_{hs} = Horizontal acceleration of soil mass

a_{hf} = Horizontal acceleration of footing

a_{hi} = Horizontal acceleration of tank as input motion

B = Width of footing

c, d = Coefficients used in the equation (7)

D = Depth of footing below soil surface

e = Void ratio

F_h = Horizontal inertial force

F_v = Vertical inertial force

g = Value of acceleration due to gravity

k_{hs} = Horizontal acceleration coefficient of soil mass

k_{hf} = Horizontal acceleration coefficient of footing

k_{hi} = Horizontal acceleration coefficient of tank as input motion

R^2 = Coefficient of determination for a estimated trend line

W = Weight of failure mass of soil

References

Al-Homoud, Azm S. and Al-Maaitah, Omar N. (1996): ‘An Experimental Investigation of Vertical Vibration of Model Footings on Sand’, *Journal of Soil Dynamics and Earthquake Engineering,* 15, pp. 431-445.

Barkan, D.D. (1962): *Dynamics of Bases and Foundations*, McGraw-Hill Book Co.

Brüel & Kjaer Sound and Vibration Measurement A/S PULSE, (2003): ‘Getting Started’ User Manual.

Knappett, J.A., Haigh, S.K. and Madabhushi (2006): ‘Mechanisms of Failure for Shallow Foundations under Earthquake Loading’, *Journal of Soil Dynamics and Earthquake Engineering,* 26 (2-4), pp. 91-102.

Liu, L., and Dobry, R. (1997): ‘Seismic Response of Shallow Foundation on Liquefiable Sand’, *Journal of Geotechnical and Geoenvironmental Engineering,* 123(6), pp. 557 – 567.

Maugeria,M., Musumeci, G., Novita, D. and Taylor, C.A. (2000): ‘Shaking Table Test of Failure a Shallow Foundation Subjected to An Eccentric Load’, *Journal of Soil Dynamics and Earthquake Engineering,* 20, pp. 435-444.

Paul, S. and Dey, A.K. (2005): ‘Behaviour of Foundations under Seismic Forces : An Overview’, *Proceedings of the Indian Geotechnical Conference,* Ahmedabad, Vol. I, pp. 345 – 348.

Paul, S. and Dey, A.K. (2006): ‘Dynamic Properties and Liquefaction Potential of Silchar Soil in North-East India’, *Proceedings of the Indian Geotechnical Conference,* Chennai, Vol. II, pp. 783 – 786.

Prakash, S (1981): *Soil Dynamics*, McGraw-Hill Book Company.